NATIONAL RADIO ASTRONOMY OBSERVATORY
SOCORRO, NEW MEXICO
VERY LARGE ARRAY PROGRAM

VLA ELECTRONICS MEMORANDUM NO. 191

THE SECTOR COUPLER - THEORY AND PERFORMANCE

J. W. Archer, M. Ogai* and E. M. Caloccia**

January 1980

ABSTRACT

The sector coupler is a high performance, broadband directional coupler for overdimensioned, millimeter wavelength, $TE_{[01]}$ mode circular waveguide communications systems. The simple mechanical construction of the device, together with its very low insertion loss, high return loss and low higher-order $TE_{[0n]}$ mode coupling in the main line, make it ideally suited to applications where many directional couplers must be installed in a long waveguide run.

*Furukawa Cable Co., Tokyo, Japan
**Raytheon, Inc., Missile Systems Div., Bedford, MA

I. INTRODUCTION

The millimeter wavelength $TE_{[01]}$ mode circular waveguide system, installed at the site of the Very Large Array in central New Mexico, carries information modulated onto a millimeter wavelength carrier in the frequency range 26.4 to 52 GHz between the many antennas in the array and the central Control Building (Weinreb et al. 1977, Archer et al. 1979). A single, low-loss, 60-mm diameter, helix-lined circular waveguide line is installed, running the full length of each arm of the array. Broadband directional couplers are installed in the main waveguide line at each antenna station to couple power to and from the main guide. The antenna waveguide system is comprised of approximately 40 meters of 20-mm diameter helix-lined circular waveguide, which includes rotary joints, rigid and flexible waveguide sections, connected to a transmit/ receive modem operating within any given 1-GHz bandwidth channel in the 26.4-GHz to 52-GHz range.

The coupling values required may vary between -23 dB and -10 dB, depending upon the transmission frequency and the distance from the central Control Building to the antenna station. However, because the spatial distribution of stations for optimum array configurations results in a greater number of stations within a relatively short distance from the Control Building, most of the couplers have coupling of less than -20 dB. The couplers exhibit very low return loss and higher-order $TE_{[0n]}$ mode coupling in the forward and reverse directions in the main line, in order to minimize amplitude and phase distortion of the primary $TE_{[01]}$ mode transmission response. Furthermore, since no repeaters are used in the communication system, with 23 couplers installed over the 20-km length of line, the magnitude of the $TE_{[01]}$ mode insertion loss of the coupler also has a significant impact on system performance.

With respect to the coupled arm of the device, when transmitting power from an antenna into the trunk waveguide, both the $TE_{[01]}$ mode reflection coefficient and the $TE_{[01]}$ to $TE_{[0n]}$ mode coupling must be small, so as to minimize distortion of the $TE_{[01]}$ mode transfer function. A detailed discussion of these performance specifications is given by Weinreb et al. (1977) and Archer (1978).

2

II. THE SECTOR COUPLER - PHYSICAL DESCRIPTION

The directional couplers used in the VLA communication system are of mechanically simple construction, yet exhibit very broadband performance. The basic premise, upon which the design of the device is based, is that the electric field distribution of $TE_{[0n]}$ modes in waveguide of circular cross section remains unperturbed when an infinitesimally thin, perfectly conducting sheet is placed perpendicular to the field lines in a diametrical plane of the guide. In fact, any two such radial planes intersecting at the center line of the cylinder, with arbitrary included angle, also leave the electric field pattern unchanged.

Such a configuration can be said to result in the formation of a pair of 'sector' waveguides, with the composite field pattern of the pair identical to that of the original circular waveguide. However, in these sector waveguides, only the characteristics of the $TE_{[0n]}$ and $TM_{(0n)}$ modes are similar to those of the corresponding modes in normal circular waveguide. Ideally, power in a $TE_{[0n]}$ mode incident on a transition from ordinary circular waveguide to the sector waveguide composite will propagate forward without reflection or mode conversion. The proportion of the incident power coupled into each sector waveguide is directly proportional to the ratio of the angles subtended by the sectors.

In the sector coupler, power coupled to the sector waveguide of smaller subtended angle is fed to an external waveguide port, whereas power coupled to the larger sector is reconverted to the normal circular electric modes of the main waveguide by gradually tapering the angle subtended by the smaller sector to zero. Several methods can be devised to change the direction of signal flow in the smaller angle sector waveguide and couple the power to a third external waveguide port. Of these, the most physically compact for a given change in angle relative to the axis of the main guide (separation angle) employs a plane, perfectly conducting mirror in the sector waveguide to transform the incident field of one sector waveguide to that of a complementary one oriented at the desired separation angle. The sector $TE_{[01]}$ mode is then transformed to the semicircular guide

3

$TE_{[01]}$ mode in an angular taper transition. Finally, power is reconverted to the circular $TE_{[01]}$ mode at an abrupt semicircular-to-circular junction in which the second semicircular port is terminated.

The complete concept is illustrated in Figure 1. The evident mechanical simplicity of the device enables the manufacture of many units with repeatable performance characteristics. However, the straightforward mechanical design belies the complex nature of the electrical performance of the sector coupler. In order to explain the electrical behavior of the device, a theoretical analysis of the abrupt sector-to-circular waveguide transition, the angular taper sector-to-semicircular transition and the abrupt change in angular orientation of the sector waveguide at a reflecting surface in the guide must be undertaken.

III. THEORETICAL ANALYSIS

The normal modes of sector waveguide of radius a may be expressed in terms of unique mode functions (Iiguchi 1959). If the angle subtended by the sector waveguide is defined by $\phi = \pm \psi$ in polar coordinates (r,ϕ), then for transverse electric $(TE_{[mn]})$ modes, the appropriate mode function, is

$$T_{[mn]} = - \sqrt{\frac{\varepsilon_m}{\psi}} \frac{1}{\sqrt{K^2_{[sn]} - s^2}} \frac{J_s(X_{[sn]}r)}{J_s(X_{[sn]}a)} \cos s\phi$$

and for transverse magnetic $(TM_{(mn)})$ modes

$$T_{(mn)} = - \sqrt{\frac{\varepsilon_m}{\psi}} \frac{1}{K_{(sn)}} \frac{J_s[X_{(sn)}r]}{J_{s+1}[X_{(sn)}a]} \sin s\phi$$

where

4

① MAIN TE_{01} MODE WAVEGUIDE
② COUPLED TE_{01} MODE WAVEGUIDE
③ SECTOR SEPTUM
④ SECTOR MIRROR
⑤ SECTOR SEMICIRCULAR (∇-◯)
⑥ SECTOR-CIRCULAR (∽-◉) TRANSITION
⑦ SEMICIRCULAR - CIRCULAR TRANSITION
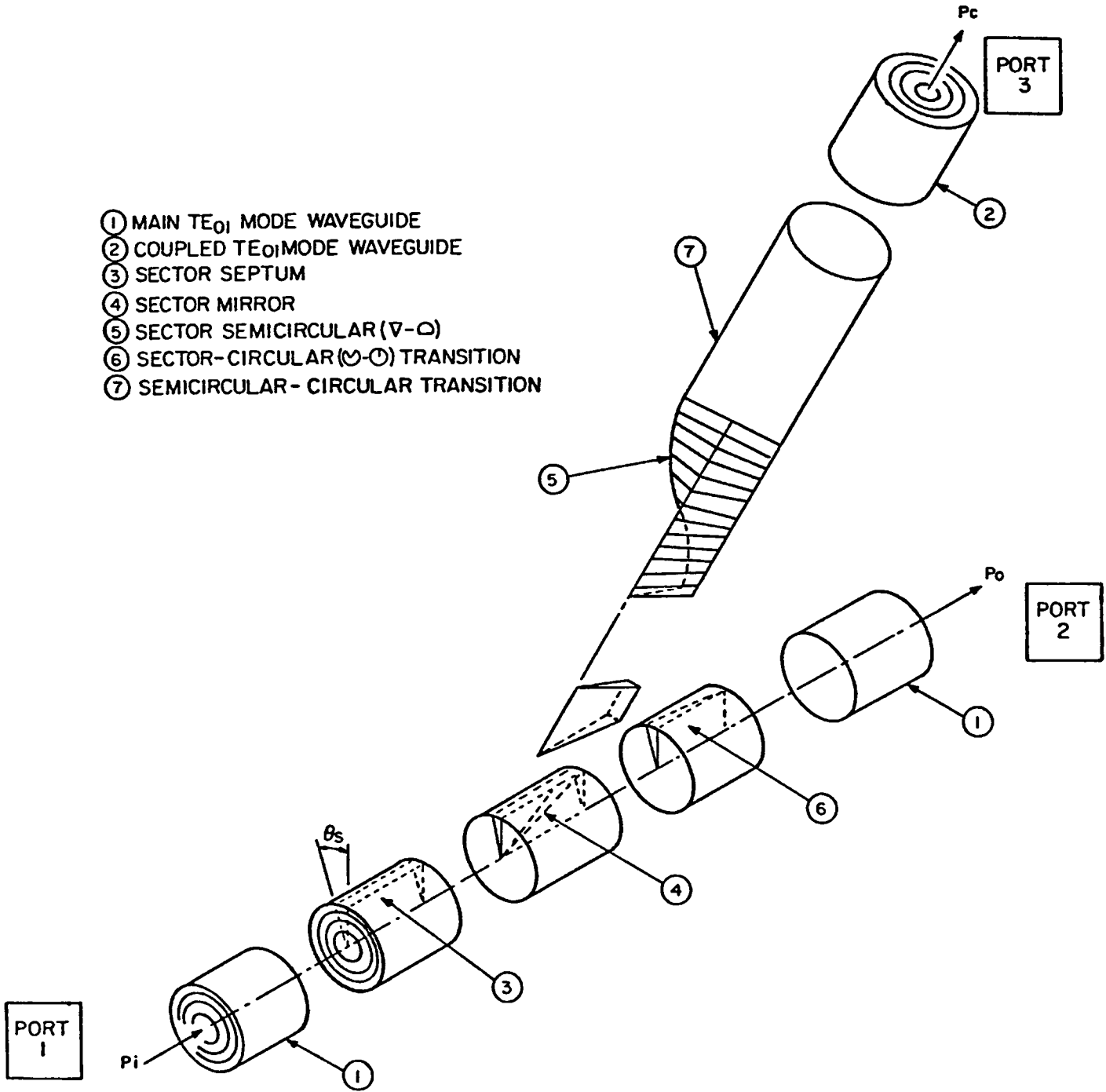
Figure 1: The sector coupler concept.

5

$$\varepsilon_m = \left\{ \begin{matrix} 2 & \text{if } m \neq 0 \\ 1 & \text{if } m = 0 \end{matrix} \right. \qquad s = \frac{m\pi}{\psi}$$

$K_{[sn]}$ is the nth root of $J_s{}'(\alpha) = 0$

$K_{(sn)}$ is the nth root of $J_s(\alpha) = 0$

$\chi_{sn} = K_{sn}/a$

Using these mode functions, the transverse electric ($\underset{\sim}{e}$) and magnetic fields ($\underset{\sim}{h}$) in a given waveguide may be written as

$$\underset{\sim}{e}_{[mn]} = \underset{\sim}{i}_\phi \left(-j\beta_{[mn]} Z_{[mn]} \frac{\partial T_{[mn]}}{\partial r} \right) + \underset{\sim}{i}_r \left(j\beta_{[mn]} Z_{[mn]} \frac{\partial T_{[mn]}}{r\partial \phi} \right)$$

$$\underset{\sim}{e}_{(mn)} = \underset{\sim}{i}_\phi \left(j\beta_{(mn)} \frac{\partial T_{(mn)}}{r\partial \phi} \right) + \underset{\sim}{i}_r \left(j\beta_{(mn)} \frac{\partial T_{(mn)}}{\partial r} \right)$$

$$\underset{\sim}{h}_{[mn]} = \underset{\sim}{i}_\phi \left(j\beta_{[mn]} \frac{\partial T_{[mn]}}{r\partial \phi} \right) + \underset{\sim}{i}_r \left(j\beta_{[mn]} \frac{\partial T_{[mn]}}{\partial r} \right)$$

$$\underset{\sim}{h}_{(mn)} = \underset{\sim}{i}_\phi \left\{ j(\beta_{(mn)}/Z_{(mn)}) \frac{\partial T_{(mn)}}{\partial r} \right\} + \underset{\sim}{i}_r \left\{ -j(\beta_{(mn)}/Z_{(mn)}) \frac{\partial T_{(mn)}}{r d\phi} \right\}$$

where $\underset{\sim}{i}_\phi$, $\underset{\sim}{i}_r$ are unit vectors in the ϕ, r directions respectively

$$\beta_{mn}^2 = \left(\frac{\omega}{c} \right)^2 - \chi_{sn}^2$$

$$Z_{[mn]} = \omega\mu/\beta_{[mn]}$$

$$Z_{(mn)} = \beta_{(mn)}/\omega\varepsilon$$

a) Abrupt Circular-to-Sector Waveguide Transition

For the case where power is incident on the junction in the $TE_{[0n]}$ mode, from the circular waveguide, the power coupling ratio from circular-to-sector waveguide may easily be determined.

If the sector waveguide $T_{[0n]}$ mode functions are normalized so that

$$T_{[0n]} = \sqrt{\frac{1}{\pi}} \; \frac{1}{K_{[0n]}J_o(X_{[0n]}a)} \; J_o \; (X_{[0n]}r)$$

then the power flow in a sector waveguide of radius a, angle 2 ψ, in terms of the transverse components of the fields, is given by

$$P_{[0n]} = Re \; \{ \int_0^r \int_{-\psi}^{\psi} (\underset{\sim}{e}_{[0n]} \times \underset{\sim}{h}_{[0n]}) \cdot \underset{\sim}{i}_z \; rdrd\phi \}$$

For $TE_{[0n]}$ modes, this reduces to $\frac{\psi}{\pi}$. Since, to satisfy the field continuity conditions at the sector/circular interface, only identical $TE_{[0n]}$ modes are required to propagate in each sector portion, with power incident in the $TE_{[0n]}$ mode from the circular waveguide, the coupling ratio is, for the smaller sector ($\psi<\pi$)

$$C_1 = \frac{\psi}{\pi}$$

and for the larger sector ($\psi>\pi$)

$$C_2 = \frac{\pi-\psi}{\pi}$$

The reflection coefficient and higher-order mode coupling at the interface, under the above conditions, will ideally be zero.

7

For the case where power is incident from one or both of the sector waveguides into the circular waveguide, the situation is substantially more complex. In this case, a large number of higher-order nonsymmetric TE and TM modes are required to be excited at the interface in order to satisfy the boundary and field continuity conditions. The power coupled to the nonsymmetric modes is lost due to the high attenuation for these modes in helix-lined circular waveguide. The problem may be analyzed for the case where power is incident from one sector waveguide only - the case of both sector waveguides exciting the circular waveguide simultaneously may be treated by applying the principle of superposition.

Consider the pair of sector waveguides to lie to the left of the junction. These guides can be thought of as constituting a composite waveguide 'A', with power propagating to the right from a sector waveguide of sector angle 2ψ. The circular waveguide to the right will be labelled 'B'. Then, at the interface, the total transverse electric and magnetic fields ($\underset{\sim}{E}$ and $\underset{\sim}{H}$ respectively) may be expanded in terms of the modes of waveguide 'A' or waveguide 'B'. For waveguide 'A', mode 1 incident,

$$\underset{\sim}{E} = (1+\rho)\, a_1\, \underset{\sim}{e}_{a_1} + \sum_{i=2}^{\infty} a_i\, \underset{\sim}{e}_{a_i}$$

$$\underset{\sim}{H} = (1-\rho)\, a_1\, \underset{\sim}{h}_{a_1} - \sum_{i=2}^{\infty} a_i\, \underset{\sim}{h}_{a_i}$$

where a_i is a mode amplitude coefficient

ρ is the reflection coefficient for mode 1

$\underset{\sim}{e}_{a_i}$, $\underset{\sim}{h}_{a_i}$ represent the transverse electric and magnetic fields for the ith mode in waveguide 'A'.

For waveguide 'B'

$$\underset{\sim}{E} = \sum_{j=1}^{\infty} b_j\, \underset{\sim}{e}_{b_j}$$

8

$$\underset{\sim}{H} = \sum_{j=1}^{\infty} b_j \underset{\sim b_j}{h}$$

Applying the boundary conditions and forcing continuity of the fields at the interface, a set of linear simultaneous equations for the mode amplitude coefficients is obtained (Wexler 1967). These equations enable the mode coupling coefficients at the interface to be derived, for a given incident mode, if all modes are correctly orthogonalized. For $i = 1,...., N$

$$\rho I_2(1,i) - \sum_{j=1}^{N} \frac{b_j}{a_1} \sum_{k=2}^{M} \frac{I_2(k,j)I_2(k,i)}{I_1(k)} - \frac{b_i}{a_1} I_3(i) = -I_2(1,i)$$

also

$$\rho I_1(1) + \sum_{j=1}^{N} \frac{b_j}{a_1} I_2(1,j) = I_1(1)$$

and

$$\frac{a_i}{a_1} = - \sum_{j=1}^{N} \frac{\frac{b_j}{a_1} I_2(i,j)}{I_i(i)}$$

The coefficient integrals are

$$I_1(i) = \iint_A (\underset{\sim a_i}{e} \times \underset{\sim a_i}{h}) \cdot \underset{\sim z}{i} \, ds$$

9

$$I_2(i,j) = \iint\limits_{A} (\underset{\sim}{e}_{a_i} \times \underset{\sim}{h}_{b_j}) \cdot \underset{\sim}{i}_z \ ds$$

$$I_3(i) = \iint\limits_{B} (\underset{\sim}{e}_{b_i} \times \underset{\sim}{h}_{b_i}) \cdot \underset{\sim}{i}_z \ ds$$

The summations are truncated at N modes in waveguide 'B' and M modes in waveguide 'A' for practical reasons, resulting in a set of N + 1 linear equations. For the present case, if there are N modes to be considered in waveguide 'B', then 2 N modes will be considered in waveguide 'A'. The latter 2 N modes comprise N modes defined over the sector subtending angle 2 ψ only and N similar modes defined over the complementary sector, with corresponding type and indices to those in waveguide 'B'.

The primary analytical task in obtaining a solution to the problem is the evaluation of the coupling integrals I_1, I_2, I_3 for all modes in the coupled waveguides. Once these integrals have been evaluated, the coefficients (in general, complex) of the linear equations may be obtained and the resulting system solved by numerical techniques using a digital computer. Appendix A gives the coefficient integrals in their most reduced form. In general, closed form expressions can not be found for these integrals and resort to numerical integration is necessary.

The numerical integration routine employed modified Romberg quadrature techniques (Fairweather 1969). The Bessel functions of the first kind [$J_\nu(u)$] required in the solution were generated numerically using an integral representation formula. The system of linear equations with complex coefficients was solved by a modified Gauss elimination procedure with complete pivoting, employing iterative error minimization techniques. With all waveguide modes correctly orthogonalized, the equations are linearly independent and a solution can be found.

For a range of sector angles for the incident waveguide, forward and reverse mode coupling coefficients to the other waveguides were calculated as a function of frequency. Incident modes considered were the sector $TE_{[01]}$ and $TE_{[02]}$ modes. Figures 2, 3 and 4 pre-
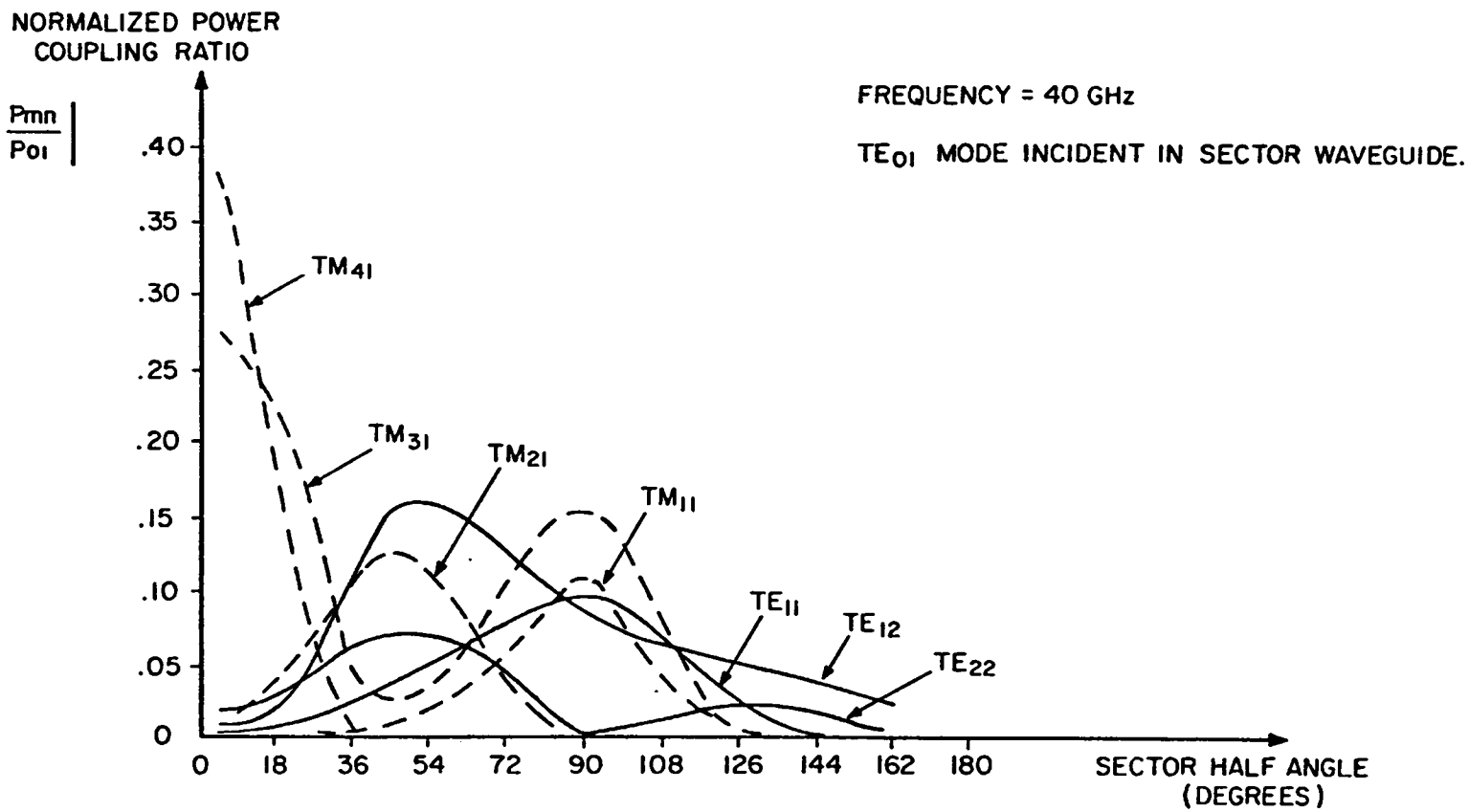
Figure 2: Power coupled to some of the modes excited in the circular waveguide at an abrupt sector/circular transition, as a function of sector angle.

11
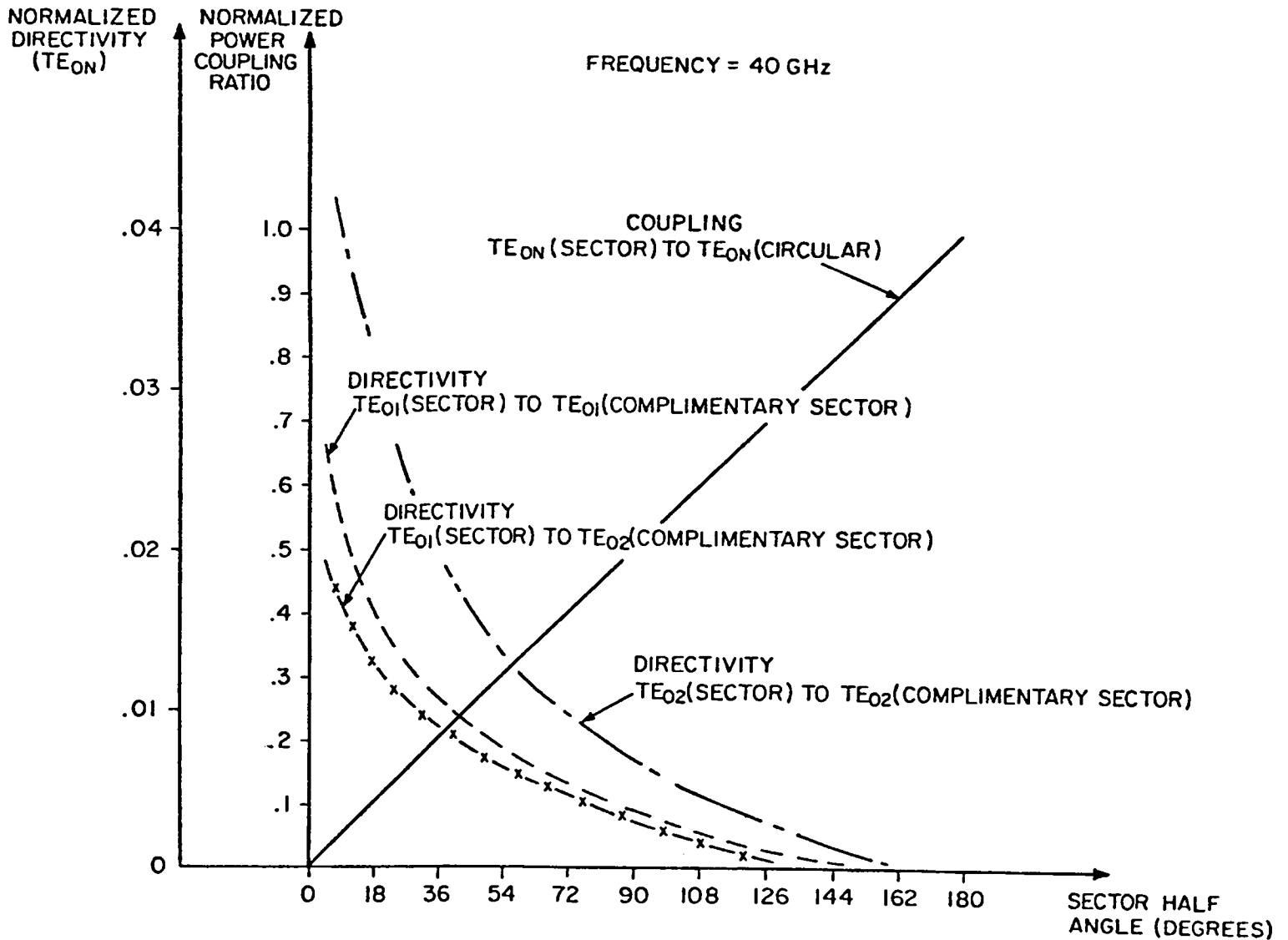
Figure 3: Predicted $TE_{[0n]}$ mode coupling at a sector/circular waveguide transition, as a function of sector angle. Note that coupling from $TE_{[01]}$ (sector) to $TE_{[02]}$ (circular) is predicted to be negligibly small.

12

VOLTAGE REFLECTION
COEFFICIENT
(INCIDENT SECTOR GUIDE)

FREQUENCY = 40 GHz

TE$_{02}$ (SECTOR)

TE$_{01}$ (SECTOR)

.35
.30
.25
.20
.15
.10
.05
0

0   18   36   54   72   90   108   126   144   162   180   SECTOR HALF
ANGLE (DEGREES)
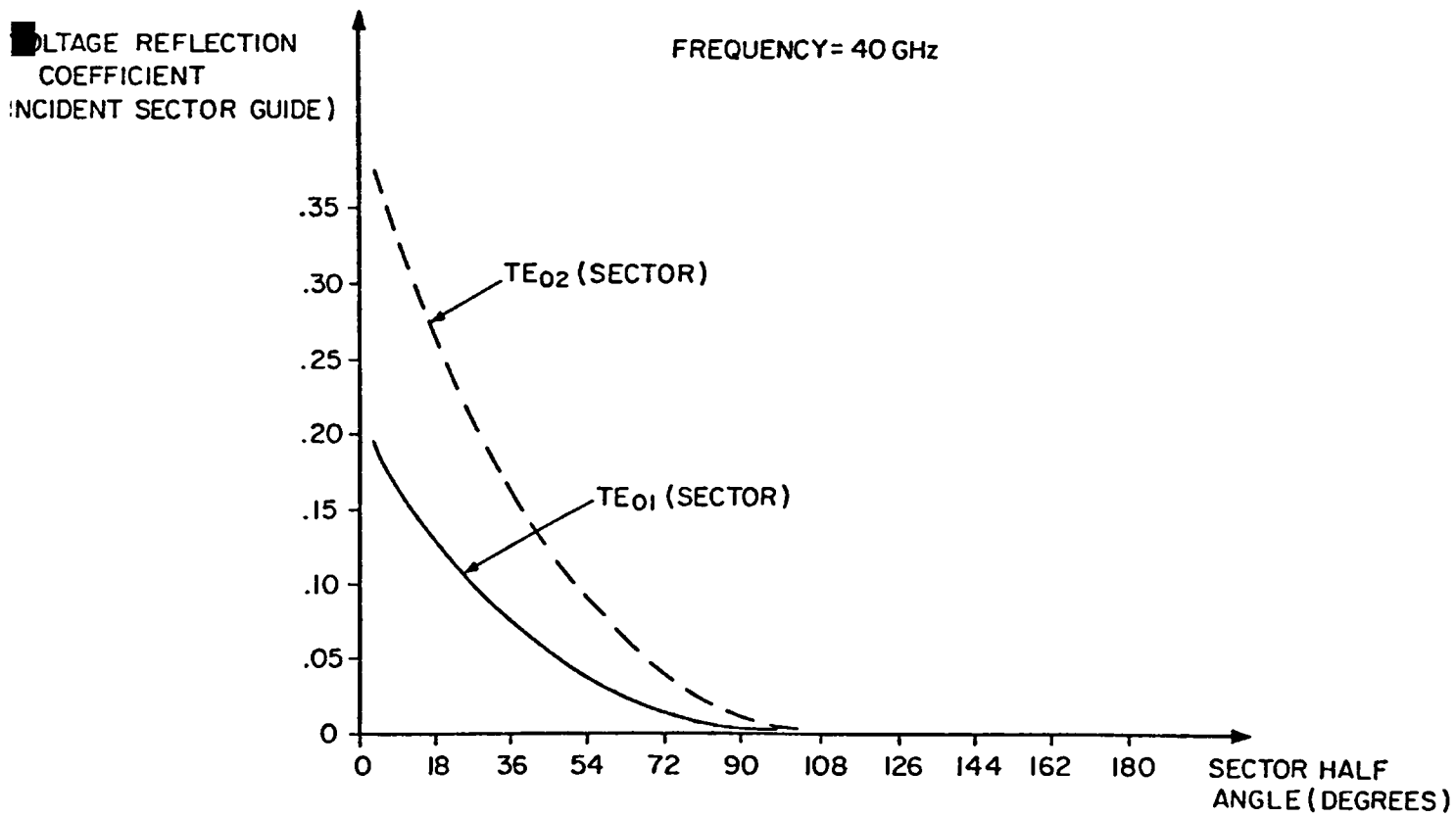
Figure 4: Predicted reflection coefficient in the sector waveguide at an abrupt sector/circular transition, at a function of sector angle.

13

sent a selection of the results of the theoretical analysis. Of primary importance, so far as the system performance of the coupler is concerned, are the coupling coefficients for the incident sector $TE_{[01]}$ mode to forward and reverse propagating $TE_{[01]}$ modes in the circular and complementary sector waveguides respectively. Also of significance are the $TE_{[01]}$ mode reflection coefficient in the sector waveguide and the $TE_{[01]}$ to $TE_{[02]}$ mode coupling coefficients for forward and reverse propagating $TE_{[02]}$ mode in the main waveguide arm.

b) The Angular Taper Sector-to-Circular Transition

In the coupled arm of the device, incident power in the sector $TE_{[01]}$ mode is first reconverted to the semicircular $TE_{[01]}$ mode and then to the circular $TE_{[01]}$ mode at an abrupt sector/circular transition in which the complementary sector waveguide is terminated. The change in sector angle may be accomplished by changing the angle linearly as a function of axial distance. A sector angle transducer of this nature, while relatively simple to fabricate, results in mode conversion between $TE_{[0n]}$ modes and numerous higher-order $TE_{[mn]}$ and $TM_{(mn)}$ ($m \neq 0$) modes. As a consequence the $TE_{[0n]}$ mode loss through the transition is greater than that due to copper losses alone if the power in the spurious modes is subsequently dissipated in a length of helix-lined waveguide.

To predict the magnitude of the mode coupling coefficients from $TE_{[01]}$ to $TE_{[mn]}$ and $TM_{(mn)}$ modes in this kind of transition requires first that Maxwell's equations be expressed in oblique coordinates, which is the natural system for a helix taper. Expressing the transverse electric and magnetic fields of the sector waveguide in terms of the normal mode functions $T_{[mn]}$, $T_{(mn)}$, inhomogeneous second order linear differential equations may be obtained relating the amplitudes of the $TE_{[01]}$ and $TE_{[mn]}$, $TM_{(mn)}$ modes in the angular taper (Iiguchi 1959 and Sporleder and Unger 1979). To achieve a solution, reciprocity is invoked, so that, in fact, coupling from an incident $TE_{[mn]}$ or $TM_{(mn)}$ mode to the $TE_{[01]}$ modes is calculated. Furthermore, the power of the incident modes is assumed to be con-

14

stant along the taper (or alternatively the coupling to secondary modes is assumed to be weak) and conversion-reconversion mechanisms are neglected.

If the angular taper is described by the equation

$$\Phi = \frac{z}{T}$$

where Φ is the sector half angle at axial position z, then the formulas for the mode coupling coefficients are

For the $TE_{[mn]}$ mode

$$C_{[mn]} = \frac{1}{2\sqrt{\beta_{[01]}}} \int_{z_1}^{z_2} \sqrt{\beta_{[mn]}} \; g(z) \; \exp\{j \int_{z_1}^{z} (\beta_{[mn]} - \beta_{[01]})dz'\} \; dz$$

For the $TM_{(mn)}$ mode

$$C_{(mn)} = \frac{c}{2\omega \; \beta_{[01]}^{3/2}} \int_{z_1}^{z_2} \sqrt{\beta_{(mn)}} \; \{\beta_{[01]}^2 \; h_1(z) + (\frac{\omega}{c})^2 \; h_2(z)\} \cdot$$

$$\exp\{j \int_{z_1}^{z} (\beta_{(mn)} - \beta_{[01]}) \; dz'\} \; dz$$

where $(z_1 - z_2)/T = \Delta\Phi$

$\Delta\Phi$ change in sector angle over taper length

$\beta_{mn}(z) = \{(\frac{\omega}{c})^2 - \chi_{sn}^2(z)\}^{\frac{1}{2}}$

ω is the radian frequency

c is the velocity of light

The functions $g(z)$, $h_1(z)$ and $h_2(z)$ may be written as

$$g(z) = \frac{T}{z^2} \iint_A \left[\frac{1}{r}\frac{\partial T_{[mn]}}{\partial \phi} + \frac{\partial}{\partial r}\left(\frac{1}{r}\frac{\partial T_{[mn]}}{\partial \phi}\right)\right] \frac{\partial T_{[01]}}{\partial r} \, r\phi dr d\phi$$

$$h_1(z) = \frac{\chi^2_{(sn)}T}{z^2} \iint_A T_{(mn)} \frac{\partial T_{[01]}}{\partial r} \, r^2 \phi dr d\phi$$

$$h_2(z) = \frac{T}{z^2} \iint_A \left[\frac{\partial T_{(mn)}}{\partial r}\{1 - 3\chi^2_{(sn)}(\frac{c}{\omega})^2\}\right.$$

$$+ \left. r^2 \frac{\partial^2 T_{(mn)}}{\partial r^2}\{1 - \chi^2_{(sn)}(\frac{c}{\omega})^2\}\right] \frac{\partial T_{[01]}}{\partial r} \, r\phi dr d\phi$$

Similar expressions may be derived for coupling with the $TE_{[02]}$ mode.

The equations were integrated numerically to give the coupling coefficients between either the $TE_{[01]}$ or $TE_{[02]}$ modes and the $TE_{[11]}$, $TE_{[21]}$, $TE_{[31]}$, and $TM_{[11]}$ modes as a function of frequency and initial sector angle, for tapers to 180°, with $T = .1612$ m/rad. The results of these computations are presented graphically in Figures 5 and 6. These curves enable the excess $TE_{[01]}$ mode insertion loss of the transition, due to mode coupling, to be predicted.

c) Sector Waveguide Corner Reflector

Power coupled to the sector waveguide from the main trunk waveguide undergoes an abrupt change in direction at a plane, perfectly reflecting surface, as shown in Figure 1. The incident electromagnetic fields of the sector waveguide are transformed at the junction to the fields of a complementary guide oriented at the desired separation angle. Although experimental measurements indicate that this type of junction possesses low TE_{01} mode insertion loss and acceptably small $TE_{01} \to TE_{02}$ mode coupling, the very complex bound-

Figure 5: Mode coupling in a sector/semicircular angular taper transition. Initial sector angle 9°, T = .1612 m/rad, $TE_{[01]}$ mode incident.

MAGNITUDE OF
MODE COUPLING
COEFFICIENT
(dB)
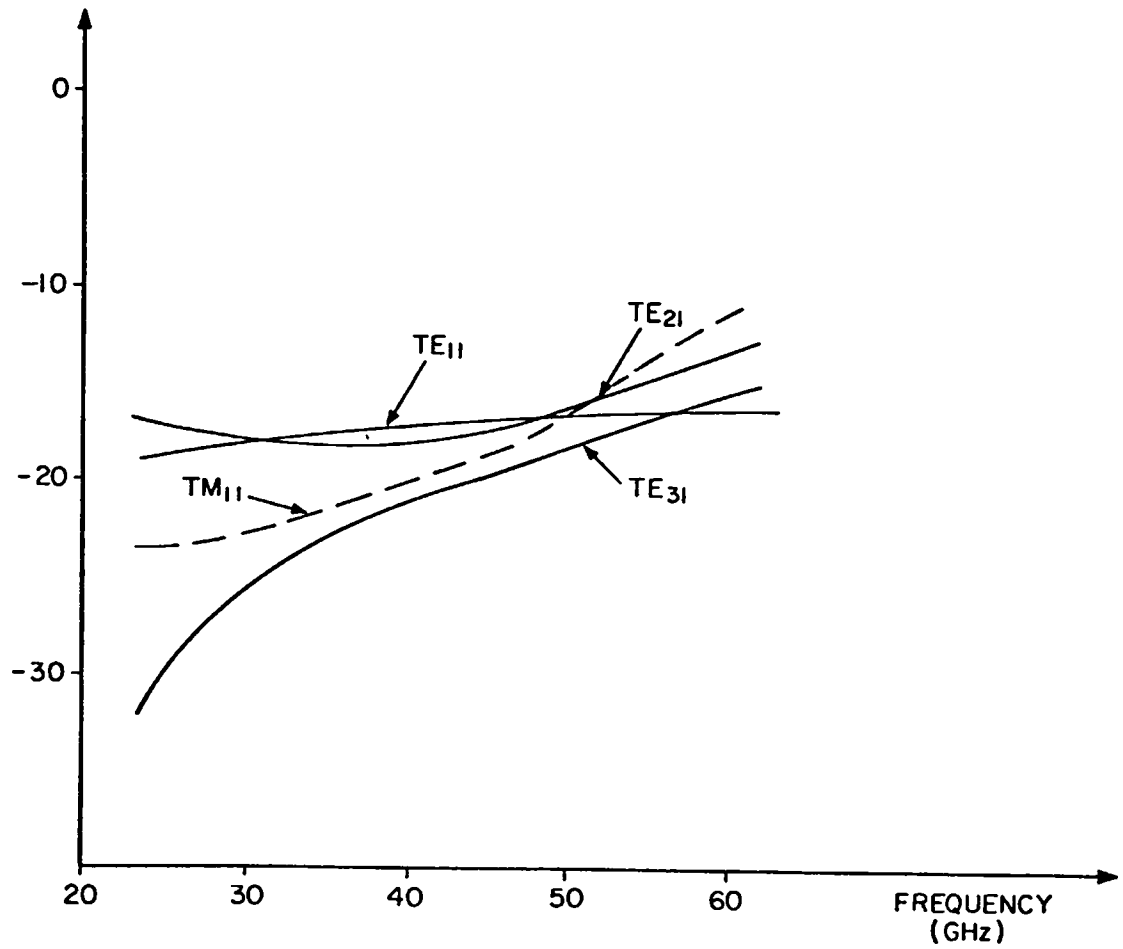
Figure 6: Mode coupling in a sector/semicircular angular taper transition. Initial sector angle 9°, T = .1612 m/rad, $TE_{[02]}$ mode incident.

ary conditions for the fields in the vicinity of the reflecting surface preclude an exact analysis. Furthermore, the approximate analytical methods used by Marcatili (1964) in analyzing the geometrically similar problem of a circular waveguide corner reflector cannot be applied here because of a lack of symmetry in the sector waveguide structure.

An attempt to formulate an analytical approach to the problem of the sector waveguide corner reflector using the results of antenna theory is outlined here. The analysis gave results which are in general agreement with experimental data, even though gross simplifying approximations were made in specifying the boundary conditions at the reflecting surface. Kirchoff's scalar field formulation of Huygens principle was applied, integrating over the current distribution over interior surface of the waveguide, to calculate the electric field distribution $E(r',0)$ in the coupled sector waveguide as a function of radius r' for $\phi = 0$. The current distributions J_s over each plane surface S_i of the waveguide junction were derived by independently calculating the electric field at each surface due to the field in the incident sector waveguide assuming no reaction of the walls on each other or on the aperture. Clearly, this approach can only yield an imperfect approximation to the true current distribution at the guide walls, since the aperture and reflecting surfaces are not significantly larger than several wavelengths in dimension at the operating frequency. A more precise analysis is, however, an extremely difficult task.

Having evaluated the approximate current distribution at the corner reflector surface and at the sector waveguide walls, the contribution to the scalar electric field, $E(r',0)$, by direct radiation from the input sector waveguide aperture and radiation from each boundary surface may be calculated independently and the resultant field obtained by superposition. The analysis commences with the assumption that the transverse fields in the aperture of the sector waveguide from which power is incident are those of the $TE_{[01]}$ mode. The surface current distributions are then independently calculated and the integrations for the resultant field performed numerically.

19

Mode coupling at the junction is analyzed by expressing the derived normalized field distribution as a linear combination of normal mode functions for the $TE_{[0n]}$ modes in sector waveguide, with $\phi = 0$. The coefficients of this series can be used to predict the magnitude of the coupling from $TE_{[01]}$ to $TE_{[0n]}$ modes in the corner waveguide junction. This method clearly neglects possible coupling to other $TE_{[mn]}$ and $TM_{(mn)}$ modes. However, the nature of field distributions derived for $\phi \neq 0$ suggests that coupling to these modes is small compared to $TE_{[01]}$ to $TE_{[0n]}$ mode interactions, at least to the order of the approximations made in the analysis. Figure 7 shows predicted $TE_{[01]}$ to $TE_{[0n]}$ mode coupling coefficients and also gives an estimate of $TE_{[01]}$ mode insertion loss at the junction due to mode coupling losses.

VI. PREDICTED AND MEASURED PERFORMANCE

a) Predictions of the Performance Characteristics

The behavior of the complete sector coupler may be predicted on the basis of the foregoing theoretical analysis of the component parts of the device. The significant aspects of coupler performance and the relevant theoretical considerations are outlined below. Figures 8 and 9 illustrate the predicted and experimental dependence of these performance parameters on frequency and also their relationship to principal sector angle $(2 \psi; \psi < \pi/2)$ at a frequency of 40 GHz.

i) $TE_{[01]}$ Mode Main Line Insertion Loss and Return Loss

The main line insertion and return loss may be predicted for a given coupler on the basis of the analysis of the abrupt sector-to-circular waveguide transition. A small direction dependence is predicted in these parameters depending upon which port is considered the input. This results from direction dependent variation in coupling losses and reflection coefficients at the sector-to-circular waveguide interface.
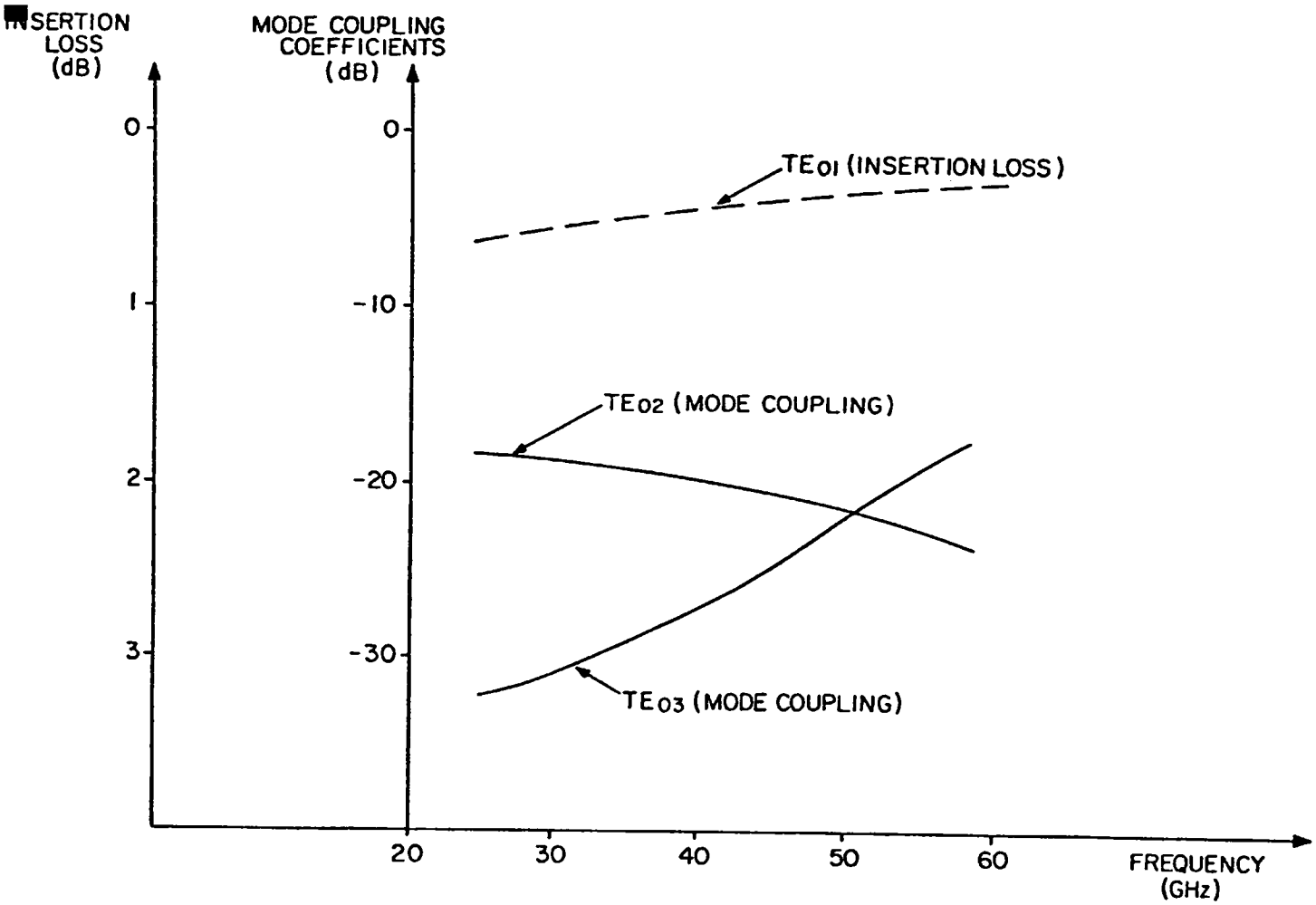
Figure 7: Predicted mode coupling coefficients for the sector wave-guide corner reflector transition with $TE_{[01]}$ mode incident. Separation angle 90°, sector angle 9°.
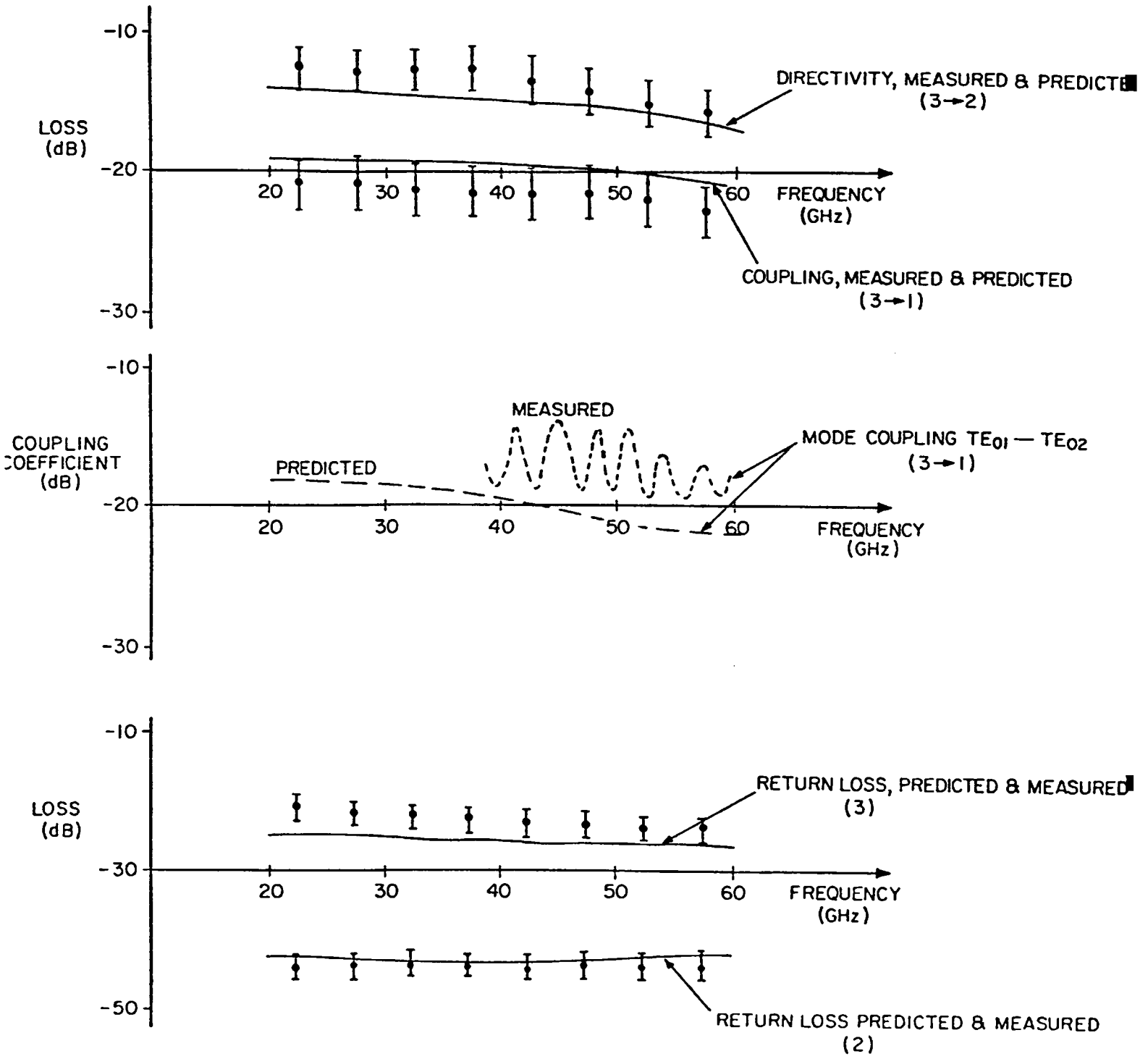
Figure 8: Comparison of predicted and measured performance of a large sample of sector couplers with sector angle of 9°. Main line insertion loss (ports 1→2) is less than 0.15 dB between 26.5 and 60 GHz. Numbers in brackets identify coupler ports concerned with the given parameter (refer to Figure 1).
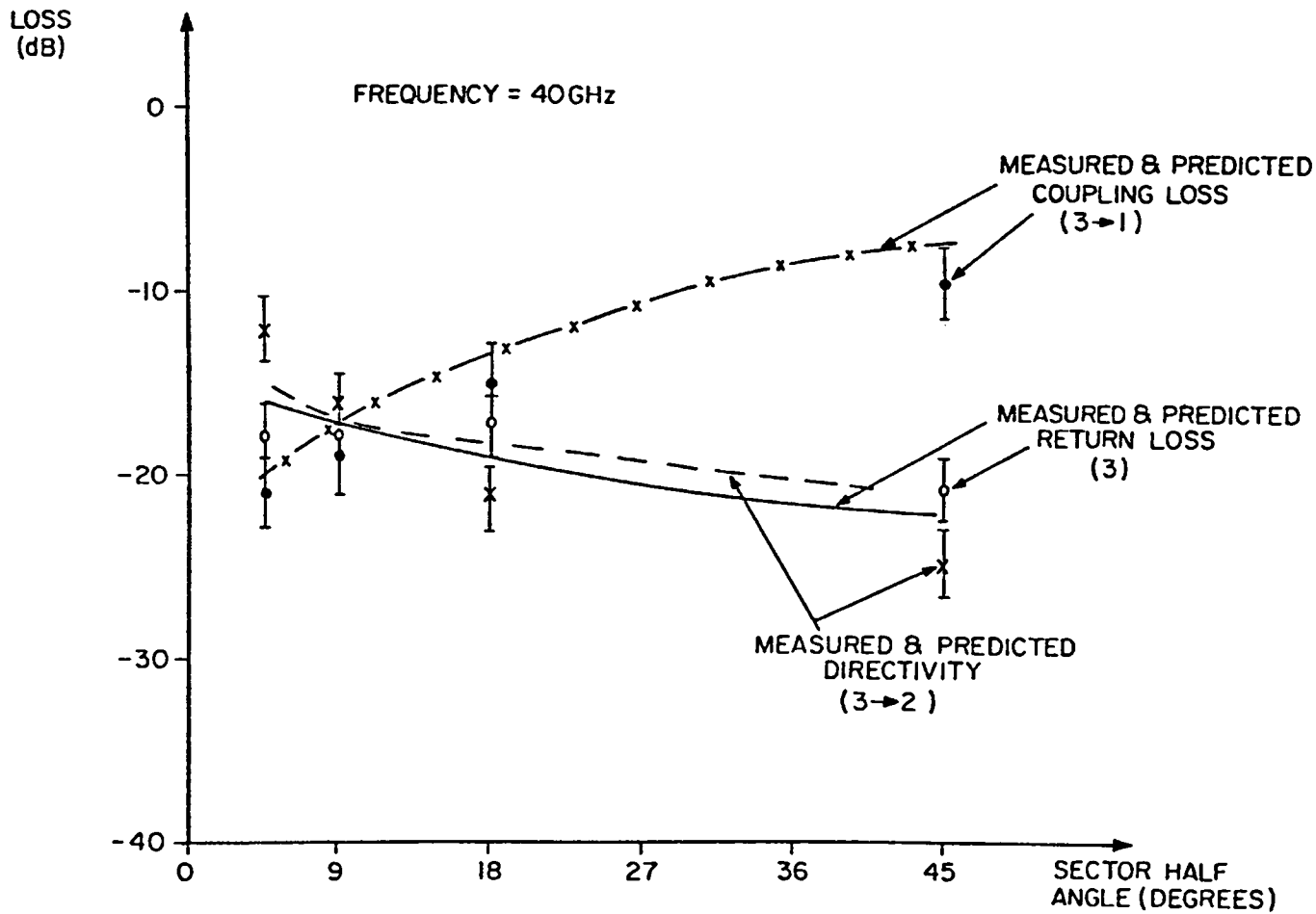
Figure 9: Some sector coupler performance parameters plotted as a function of sector half angle.

ii) $TE_{[01]}$ Mode Coupling Loss and Directivity for the Coupled Port

The coupling loss is influenced by three mechanisms in the sector coupler. The sector angle ratio is the principal determinant of coupling for a given coupler. Additional losses are contributed by the sector waveguide corner reflector, sector-to-semicircular angular taper transition and the abrupt semicircular-to-circular waveguide junction in the coupled arm. Directivity, however, depends only upon the geometry of the abrupt sector-to-circular waveguide transition in the main trunk waveguide.

iii) $TE_{[01]}$ to $TE_{[0n]}$ Mode Coupling in the Coupled Arm

Interactions between circular electric modes in the coupled arm of the device can be considered to result from two mechanisms. The principal source of direct coupling is, as predicted theoretically, the sector waveguide corner junction. However, the experimental results indicate that the coupled arm mode coupling response exhibits a quasi-periodic variation (of small amplitude) about a nominal coupling value. The nonuniformity in the coupling response is thought to arise from second-order mode coupling ($TE_{[02]} \rightarrow [TE_{[mn]}, TM_{(mn)}] \rightarrow TE_{[01]}$) in the sector-to-semicircular waveguide angular taper, since results for different taper lengths (different taper constant) indicate that the effect is greater, and the periodicity larger, for short tapers, in which the general level of mode coupling is higher. The approximate theoretical analysis of Section IIIb neglected secondary conversion-reconversion mechanisms and thus could not predict the observed effect. For a taper length of .24 meters the coupling mechanism due to secondary interactions may be approximated by a $TE_{[01]}$ to $TE_{[02]}$ mode coupling discontinuity with coupling coefficient -20 dB located approximately .20 meters from the sector waveguide corner reflector junction.

iv) $TE_{[01]}$ Mode Return Loss in the Coupled Arm

For power incident at the coupled arm of the coupler the principal source of reflection is the abrupt sector-to-circular transition in

24

the main waveguide. The incident and reflected signals are modified by the additional losses in the coupled arm signal path as outlined in ii), resulting in a significantly better return loss at the input to the coupled port than would be predicted due to $TE_{[01]}$ mode reflections at the abrupt transition alone.

v) $TE_{[0n]}$ Mode Generation in the Main Line

For power incident from either of the main trunk waveguide ports, higher-order circular TE mode coupling is in general very small, as predicted by the analysis of Section IIIa. For power incident from the coupled port, forward coupling to higher-order modes in the main circular waveguide is also negligible. However, the theory predicts a small, but significant, reversing coupling of higher-order modes into the complementary sector waveguide.

b) Measured Performance Statistics

More than sixty sector couplers, with varying degrees of coupling, have been fabricated, tested and installed in the waveguide communication system at the VLA Site. The measured points shown in Figures 8 and 9, therefore, represent mean performance of a large sample of devices. The error bars in the figure denote the peak deviation from the mean of a given performance measure over the sample space. Experimental errors have been assumed negligible compared with the scatter in performance of such a large sample of couplers. It can be seen that the theoretically predicted behavior is in reasonable agreement with the measured performance. The fact that the theoretical treatment neglects copper losses in the waveguides possibly accounts for the small discrepancies between predicted and measured loss values. Clearly, the sector coupler behavior is sufficiently well understood theoretically to enable the effects of the variables in the design to be adequately evaluated.

V. CONCLUSION

An analytical approach to the evaluation of a novel type of directional coupler for overdimensioned circular waveguide has been out-

25

lined. Adequate agreement between theory and experiment has been demonstrated. The directional couplers are of mechanically simple construction, yet exhibit very low insertion loss, high return loss and low higher-order $TE_{[0n]}$ mode coupling in the main line. These performance characteristics as well as the broad constant-coupling bandwidth make the sector coupler ideally suited to applications in broadband waveguide communications systems where many directional couplers must be installed in the waveguide line.

APPENDIX I

Coefficient Integrals for Sector-to-Circular
Waveguide Junction Mode Coupling Equations

a) The integrals I_1, I_3 are of the form

$$I = \iint_S \underset{\sim}{e}_s \times \underset{\sim}{h}_s \cdot \underset{\sim}{i}_z \, ds$$

where S is the cross section over which the integration is to be performed.

   i) For $TE_{[mn]}$ modes in sector waveguide of included angle 2 ψ

   ($\psi = \pi$ for I_3)

$$I = - \frac{\varepsilon_m \psi \beta^2_{[sn]} N^2_{[sn]} Z_{[sn]} a^2}{2 K^2_{(kn)}} \{1 - (\frac{S}{K_{[sn]}a})^2\} J^2_s(K_{[sn]}a)$$

   ii) For $TM_{(mn)}$ modes in sector waveguide of included angle 2 ψ

$$I = \frac{-\varepsilon_m \psi \beta^2_{(sn)} N^2_{(sn)} Z_{(sn)} a^2}{2 K^2_{(sn)}} J'^2_s(K_{(sn)}a)$$

b) The integrals I_2 cannot, except for certain mode pairs, be expressed in closed form. These integrals are of the form

$$I = \iint_{S_1} \underset{\sim}{e}_{s_1} \times \underset{\sim}{h}_{s_2} \cdot \underset{\sim}{i}_z \, ds$$

where S_1 and S_2 are the cross sections of the waveguide pair forming the function. Power is incident from S_1, a sector waveguide of included angle 2 ψ.

27

i)   For $TE_{[mn]}$ modes in S_1, $TE_{[pq]}$ modes in S_2

$$K_1 = (-1)^m \frac{Z^1_{[sn]} \; \beta^{(1)}_{[sn]} \; \beta^{(2)}_{[pq]} \; N^{(1)}_{[sn]} \; N^{(2)}_{[pq]}}{K^{(1)}_{[sn]} \; K^{(2)}_{[pq]}} \cdot \frac{2p}{S^2 - p^2} \cdot \sin(p\psi)$$

$$I = K_1 \int_0^a \left\{ \frac{S^2}{K^{(1)}_{[sn]} \; K^{(2)}_{[pq]}} \frac{1}{r^2} J_S(K^{(1)}_{[sn]} r) J_p(K^{(2)}_{[pq]} r) + J_S'(K^{(1)}_{[sn]} r) J_p'(K^{(2)}_{[pq]} r) \right\} r d\blacksquare$$

(ii)   For $TM_{(mn)}$ modes in S_1, $TM_{(pq)}$ modes in S_2

$$K_2 = \frac{(-1)^m \; \beta^{(1)}_{(sn)} \; \beta^{(2)}_{(pq)} \; N^{(1)}_{(sn)} \; N^{(2)}_{(pq)}}{z^{(2)}_{(pq)} \; K^{(1)}_{(sn)} \; K^{(2)}_{(pq)}} \cdot \frac{2p}{s^2 - p^2} \sin(p\psi)$$

$$I = K_2 \int_0^a \left\{ \frac{S^2}{K^{(1)}_{(sn)} \; K^{(2)}_{(pq)}} \frac{1}{r^2} J_S(k^{(1)}_{(sn)} r) J_p(k^{(2)}_{(pq)} r) + J_S'(k^{(1)}_{(sn)} r) J_p'(k^{(2)}_{(pq)} r) \right\} r d\blacksquare$$

iii)   For $TE_{[mn]}$ modes in S_1, $TM_{(pq)}$ modes in S_2

$$K_3 = -(-1)^m \frac{Z^{(1)}_{[sn]}}{Z^{(2)}_{(pq)}} \cdot \frac{\beta^{(1)}_{[sn]} \; \beta^{(2)}_{(pq)} \; N^{(1)}_{[sn]} \; N^{(2)}_{(pq)}}{K^{(1)}_{[sn]} \; K^{(2)}_{(pq)}} \cdot \frac{2}{S^2 - p^2} \sin(p\psi)$$

$$I = K_3 \int_0^a \left\{ \frac{S^2}{K^{(1)}_{[sn]} r} J_\rho'(K^{(2)}_{(pq)} r) J_S(K^{(1)}_{[sn]} r) + \frac{p^2}{K^{(2)}_{(pq)} r} J_\rho(K^{(2)}_{(pq)} r) J_S'(K^{(1)}_{[sn]} r) \right\} r dr$$

iv)   For $TM_{(mn)}$ modes in S_1, $TE_{[pq]}$ modes in S_2

$$K_4 = (-1)^m \frac{N^{(1)}_{(sn)} \; N^{(2)}_{[pq]} \; \beta^{(1)}_{(sn)} \; \beta^{(2)}_{[pq]}}{K^{(1)}_{(sn)} \; K^{(2)}_{[pq]}} \cdot \frac{2}{S^2 - p^2} \cdot \sin(p\psi)$$

$$I = K_4 \int_0^a \left\{ \frac{p^2}{K^{(2)}_{[pq]} r} J_S'(K^{(1)}_{(sn)} r) J_\rho(K^{(2)}_{[pq]} r) + \frac{S^2}{K^{(1)}_{(sn)} r} J_S(K^{(1)}_{(sn)} r) J_\rho'(K^{(2)}_{[pq]} r) \right\} r dr$$

REFERENCES

1. Weinreb, S., Predmore, R., Ogai, M., Parrish, A., "Waveguide System for a Very Large Antenna Array", Microwave Journal, Vol. 20, No. 3, pp. 49-52, March, 1977.

2. Archer, J. W., Caloccia, E. M., Serna, R., "An Evaluation of the Performance of the VLA Circular Waveguide System", to be published, IEEE-MTT, 1980.

3. Archer, J. W., "Spurious Responses in the VLA Circular Waveguide System", NRAO-VLA Electronics Memorandum No. 177, August, 1978.

4. Iiguchi, S., "Mode Conversion in the Excitation of TE_{01} Waves in a TE_{01} Mode Transducer", Proc. Symp. MM-Waves, p. 595, Polytechnic Instit., Brooklyn, April 1-2, 1959.

5. Wexler, A., "Solution of Waveguide Discontinuities by Modal Analysis", IEEE-MTT, Vol. 15, No. 9, pp. 508-517, September, 1967.

6. Fairweather, G., "Modified Romberg Quadrature", Comm. ACM 12, p. 324, June, 1969.

7. Marcatili, E. A. J., "Miter Elbow of Circular Electric Mode", Proc. Symp. on Quasioptics, Polytechnic Instit., Brooklyn, p. 535, June, 1964.

8. Sporleder, F. and Unger, H.-G., "Waveguide Tapers, Transitions and Couplers", IEE Electromagnetic Wave Series No. 6, Chapter 7, Peter Peregrinus, Ltd., London, 1979.